Genetic Ablation of Mast Cells Redefines the Role of Mast Cells in Skin Wound Healing and Bleomycin-Induced Fibrosis

Sebastian Willenborg[1], Beate Eckes[1], Jürgen Brinckmann[2,3], Thomas Krieg[1,4,5], Ari Waisman[6], Karin Hartmann[1], Axel Roers[7] and Sabine A. Eming[1,4,5]

Conclusive evidence for the impact of mast cells (MCs) in skin repair is still lacking. Studies in mice examining the role of MC function in the physiology and pathology of skin regenerative processes have obtained contradictory results. To clarify the specific role of MCs in regenerative conditions, here we used a recently developed genetic mouse model that allows conditional MC ablation to examine MC-specific functions in skin. This mouse model is based on the cell type–specific expression of Cre recombinase in connective tissue–type MCs under control of the Mcpt5 promoter and the Cre-inducible diphtheria toxin receptor–mediated cell lineage ablation by diphtheria toxin. In response to excisional skin injury, genetic ablation of MCs did not affect the kinetics of reepithelialization, the formation of vascularized granulation tissue, or scar formation. Furthermore, genetic ablation of MCs failed to prevent the development of skin fibrosis upon bleomycin challenge. The amount of deposited collagen and the biochemistry of collagen fibril crosslinks within fibrotic lesions were comparable in MC-depleted and control mice. Collectively, our findings strongly suggest that significant reduction of MC numbers does not affect skin wound healing and bleomycin-induced fibrosis in mice, and provide to our knowledge previously unreported insight in the long-debated contribution of MCs in skin regenerative processes.

Journal of Investigative Dermatology (2014) **134,** 2005–2015; doi:10.1038/jid.2014.12; published online 30 January 2014

INTRODUCTION

Impaired wound healing and fibrosis of diverse tissues are leading causes of morbidity and mortality (Wadman, 2005; Sen *et al.*, 2009). The molecular and cellular events underlying these processes are not completely understood and require further analysis to design effective therapeutic approaches. The physiologic healing response upon excisional skin injury is initiated by a local, timely limited inflammatory response, followed by the formation of vascularized granulation tissue, myofibroblast differentiation, epithelialization, and a long-lasting phase of tissue maturation (Martin, 1997; Gurtner *et al.*, 2008). The inflammatory response has potential to cause severe tissue damage with permanent remodeling of the extracellular matrix if imbalanced, resulting in uncontrolled connective tissue deposition and function-impairing scarring (Eming *et al.*, 2007; Lucas *et al.*, 2010).

Tissue-resident mast cells (MCs) and MC precursors recruited from the circulation have been implicated in controlling the balance of inflammatory signals directing the quality of tissue repair and fibrosis. Yet, MC-specific functions in the physiology and/or pathology of the wound healing response are not clear. MC accumulation and activation at the site of skin injury and in fibrotic tissue in humans and mice is well documented (Yamamoto *et al.*, 1999a; Trautmann *et al.*, 2000; Weller *et al.*, 2006; Gabrielli *et al.*, 2009). Furthermore, a recent study in mice suggests that MCs mediate the transition from scarless to fibrotic healing during fetal development (Wulff *et al.*, 2012). To investigate the cell-specific impact of MCs during skin repair, the MC-deficient mouse line WBB6F1-Kit^{W}/Kit$^{W\text{-}v}$ (W/W^{v} mice) has been frequently used (Kitamura *et al.*, 1978). However, independent studies in tissue repair generated in W/W^{v} mice resulted in partially contradictory results. In particular, the impact of MCs on the inflammatory infiltrate, the kinetics of wound closure, induction of angiogenesis, and the development of fibrosis are under debate (Yamamoto *et al.*, 1999b; Egozi *et al.*, 2003; Nauta *et al.*, 2013). Notably, recent studies revealed that

[1]*Department of Dermatology, University of Cologne, Cologne, Germany;* [2]*Department of Dermatology, University of Lübeck, Lübeck, Germany;* [3]*Institute of Virology and Cell Biology, University of Lübeck, Lübeck, Germany;* [4]*Cologne Excellence Cluster on Cellular Stress Responses in Aging-Associated Diseases (CECAD), University of Cologne, Cologne, Germany;* [5]*Center for Molecular Medicine (CMMC), University of Cologne, Cologne, Germany;* [6]*Institute for Molecular Medicine Mainz, University of Mainz, Mainz, Germany and* [7]*Institute for Immunology, Medical Faculty Carl Gustav Carus, Dresden University of Technology, Dresden, Germany*

Correspondence: Sabine A. Eming, Department of Dermatology, University of Cologne, Kerpener Strasse 62, 50931 Köln, Germany.
E-mail: sabine.eming@uni-koeln.de

Abbreviations: APC, allophycocyanin; DT, diphtheria toxin; eYFP, enhanced yellow fluorescent protein; i.d., intradermal; i.p., intraperitoneal; iDTR, inducible diphtheria toxin receptor; MC, mast cell; Mcpt5, mast cell protease 5

Received 15 October 2013; revised 10 December 2013; accepted 12 December 2013; accepted article preview online 9 January 2014; published online 30 January 2014

© 2014 The Society for Investigative Dermatology

W/W^v mice are not only MC deficient but are also characterized by other complex alterations of their immune system that might contribute to the phenotypes observed in specific disease models (Nigrovic *et al.*, 2008). In addition to MC deficiency, W/W^v mice suffer from anemia and neutropenia, lack intraepithelial γδ T lymphocytes, and are prone to dermatitis and gastritis (Zhou *et al.*, 2007; Nigrovic *et al.*, 2008). In fact, recent studies reported on major differences in the outcome of contact hypersensitivity responses and antibody-induced arthritis between W/W^v mice and genetic mouse models of inducible and constitutive MC ablation (Dudeck *et al.*, 2011; Feyerabend *et al.*, 2011).

To determine the specific role of MCs in skin repair and fibrosis, here we used a recently developed genetic mouse model of inducible depletion of connective tissue MCs, in which no side effects have been described (Dudeck *et al.*, 2011). Our findings strongly suggest that severe reduction of MC numbers does not affect skin wound healing and bleomycin-induced fibrosis in mice.

RESULTS

Depletion of connective tissue–type MCs in wound tissue in Mcpt5Cre/iDTR mice

To analyze the functional impact of MCs during tissue repair in the skin, we generated mice in which MCs can be specifically and inducibly ablated by the application of diphtheria toxin (DT). This mouse line (Mcpt5Cre/iDTR) was generated by crossing Cre-inducible human DT-receptor-transgenic mice (iDTR) to recently generated Mcpt5Cre mice, shown to express Cre recombinase specifically in connective tissue–type MCs (Figure 1a) (Buch *et al.*, 2005; Scholten *et al.*, 2008).

To assess specificity and efficiency of Mcpt5Cre-mediated recombination in wound MCs, we first inflicted full-thickness excision wounds on the back of Mcpt5Cre/eYFP reporter mice, in which Cre-mediated excision of a STOP cassette leads to enhanced yellow fluorescent protein (eYFP) expression under control of the Rosa26 promoter (Figure 1b). Immunostainings of wound tissue for MCs ($c\text{-}kit^+$) and eYFP showed that eYFP expression within the granulation tissue was restricted to $c\text{-}kit^+$ cells, with most of $c\text{-}kit^+$ cells expressing eYFP (Figure 1c). MC accumulation at the wound site was sparse within the granulation tissue during the early (day 4) and mid (day 7) phase of repair (data not shown), and was detectable in significant numbers at the late stage (day 14) within the scar tissue (Figure 1c). FACS analysis of wound cell suspensions isolated from Mcpt5Cre/eYFP reporter mice at day 14 after injury showed that $\sim 0.9 \pm 0.1\%$ of all wound cells expressed eYFP and that $CD45^+$ cells represented the major fraction of $eYFP^+$ cells (Figure 1d). The majority of $eYFP^+$ $CD45^+$ cells were $c\text{-}kit^+IgE^+$ (90.5%), representing connective tissue MCs. Few $eYFP^+CD45^+$ cells were $c\text{-}kit^+IgE^-$ (7.2%), corresponding to MC precursors or immature MCs. These findings demonstrate that recombination within the leukocyte compartment is highly specific for MCs. We observed a minor fraction of $eYFP^+CD45^-$ cells (0.1%) (Figure 1d, lower panel) that failed to express c-kit or Fc epsilon receptor I and that were sporadically detected in the hyperproliferative epidermis of day 14 wounds. At this stage, we cannot explain this observation because keratinocytes are not known to express Mcpt5. In fact, we never detected $eYFP^+$ cells in the epidermis of uninjured Mcpt5/eYFP reporter mice. To investigate the efficiency of Mcpt5Cre-mediated recombination, we next analyzed eYFP expression within the population of $c\text{-}kit^+IgE^+$ cells. On average, $81.8 \pm 5.9\%$ of $c\text{-}kit^+IgE^+$ cells expressed eYFP (Figure 1e).

To induce MC depletion in Mcpt5Cre/iDTR mice, we followed a protocol for DT injections as previously described (Dudeck *et al.*, 2011). $c\text{-}kit^+IgE^+$ MCs in the peritoneal cavity (Figure 2a) and $Giemsa^+$ MCs in unwounded back skin (Figure 2b) in DT-injected Mcpt5Cre/iDTR mice were efficiently ablated. Consistent with the quantification of MCs ($eYFP/c\text{-}kit^+$) in wound tissue during the time course of healing in Mcpt5Cre/eYFP reporter mice, analysis of Giemsa-stained sections in control mice revealed a significant increase of MCs during the late phase of healing, thereby restoring the average MC density of unwounded skin (Figure 2d and e). In contrast, MCs within the granulation (day 7)/scar (day 14) tissue and in unwounded skin at wound edges in MC-depleted mice were significantly reduced over the entire time course of healing when compared with control mice (Figure 2d and e). Particularly, the combination of systemic (intraperitoneal (i.p.)) and local (intradermal (i.d.)) DT injections after injury (Figure 2c) leads to severe MC depletion in late-stage wounds. Reduced DT injections after injury ($1\times$ i.p. after injury) resulted in a mild MC depletion (MC reduction at day 14 after injury: $42.3 \pm 13.5\%$) (Supplementary Figure S1 online). Efficient ablation of MCs in wound tissue of DT-treated Mcpt5Cre/iDTR mice through the entire repair response was confirmed by immunohistochemical staining for c-kit and Toluidine blue staining (Supplementary Figure S2 online).

MC ablation does not affect the development of granulation tissue and epithelialization in skin wounds

To examine the functional impact of MCs during the diverse stages of repair, full-thickness skin wounds were inflicted on the back of Mcpt5Cre/iDTR and control mice, and at diverse time points after injury the healing response was assessed by macroscopical and histological morphometric analyses. MC depletion was performed following the DT injection regime outlined in Figure 2c. The macroscopic analysis of wound closure was comparable in MC-depleted and control mice (data not shown). Determining the distance between the two epithelial tips (histological measure for epithelialization) revealed that the rate of wound closure was not affected by MC ablation. Figure 3a outlines the key histological features of an early- and mid-stage wound (Figure 3b). Furthermore, the kinetics of reepithelialization and development of an early vascularized granulation tissue were independent of MCs (Figure 3b). The only significant difference between wound tissue of MC-depleted and control mice was the increased distance between the two edges of the panniculus carnosus at day 3 after injury, indicating a temporary attenuated wound contraction in MC-depleted mice (Figure 3b and c). The distance between the two edges of the panniculus carnosus is regarded as a measure of wound contraction that in rodents is a combination of contractile myofibroblasts developing

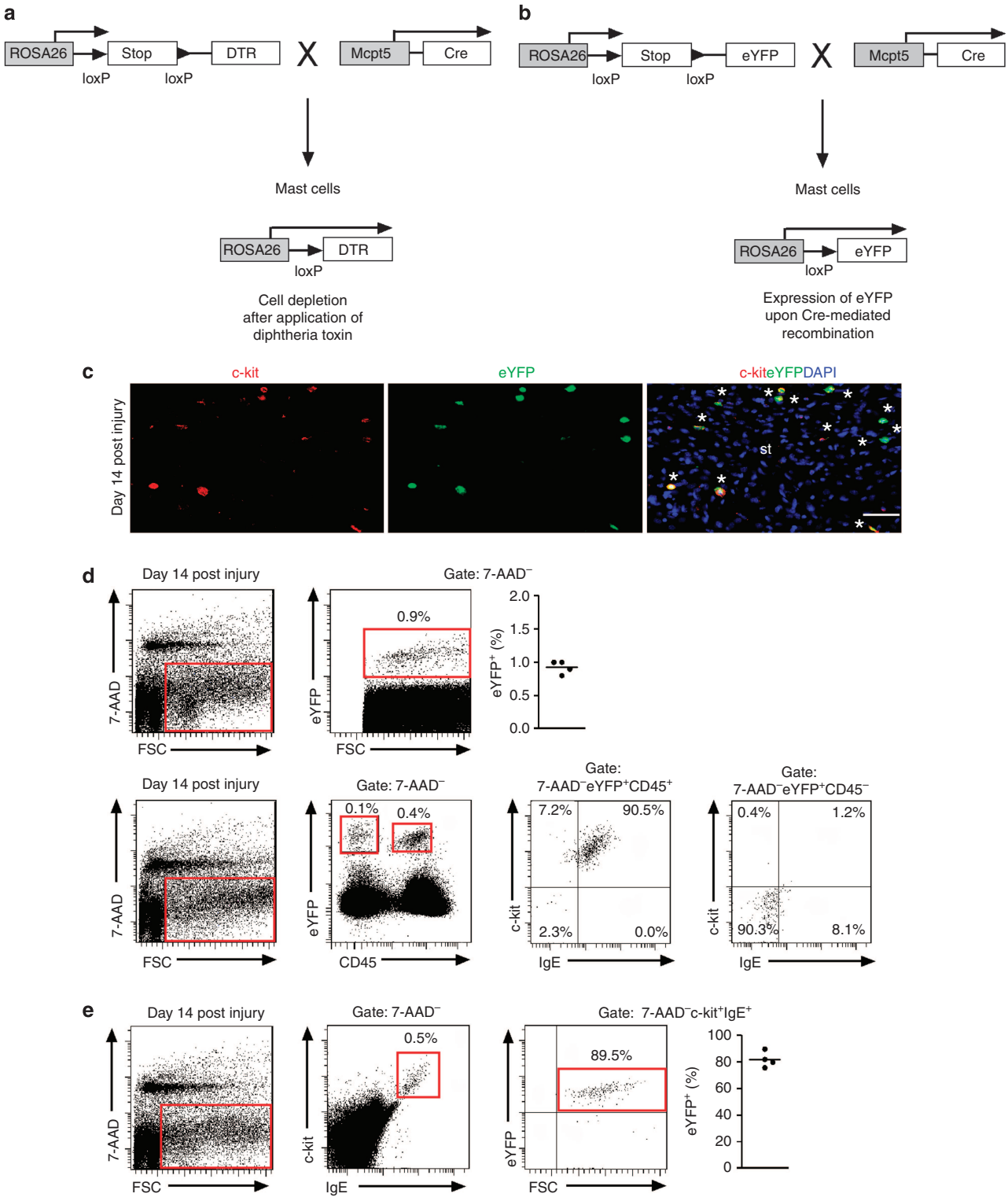

Figure 1. Gene deletion in Mcpt5Cre/eYFP mice. (**a**) Generation of Mcpt5Cre/iDTR and (**b**) Mcpt5Cre/eYFP mice. (**c**) c-kit/eYFP immunostainings of wound sections in Mcpt5Cre/eYFP reporter mice at day 14; asterisks indicate c-kit$^+$eYFP$^+$ cells; bar = 40 μm. (**d**) Specificity of Mcpt5Cre-mediated recombination: single-cell suspensions isolated from wounds at day 14 in Mcpt5Cre/eYFP reporter mice were analyzed by flow cytometry. Upper panel: 7-AAD$^-$eYFP$^+$ cells were gated and quantified; lower panel: 7-AAD$^-$eYFP$^+$CD45$^+$ or 7-AAD$^-$eYFP$^+$CD45$^-$ cells were gated and analyzed for c-kit and surface-bound IgE; each dot represents one wound ($n = 4$ wounds from 2 mice). (**e**) Efficiency of Mcpt5Cre-mediated recombination in mast cells (MCs): single-cell suspensions isolated from wounds at day 14 in Mcpt5Cre/eYFP reporter mice were analyzed by flow cytometry: 7-AAD$^-$c-kit$^+$IgE$^+$ cells were gated and analyzed for expression of eYFP; each dot represents one wound ($n = 4$ wounds from 2 mice). Two independent experiments were performed. 7-AAD, 7-Amino-Actinomycin D; eYFP, enhanced yellow fluorescent protein; iDTR, inducible diphtheria toxin receptor; Mcpt5, mast cell protease 5; st, scar tissue.

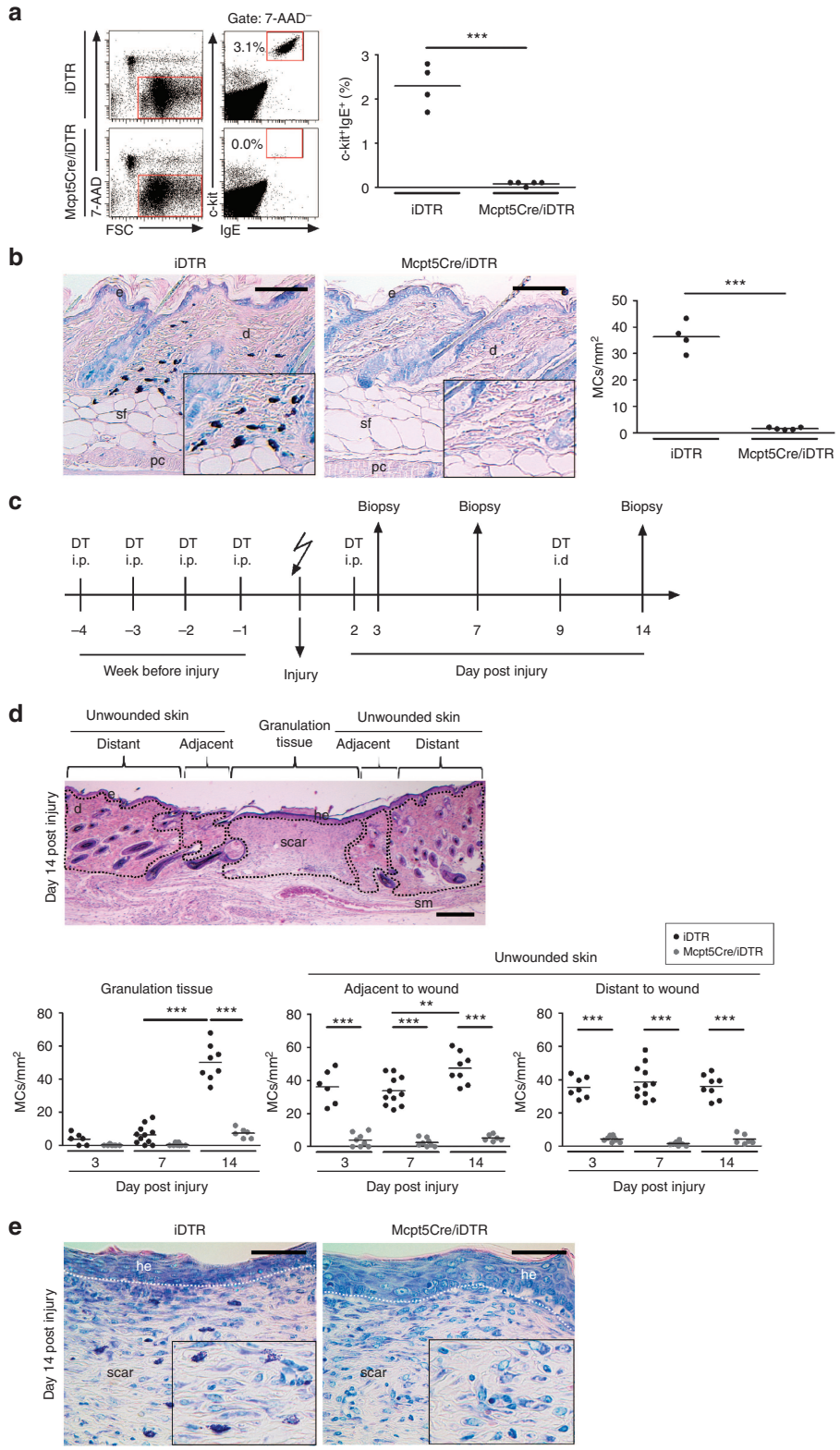

Figure 2. Efficient MC ablation in Mcpt5Cre/iDTR mice during skin wound healing. (**a**) Quantification of MCs in the peritoneal cavity after 4 intraperitoneal (i.p.) injections of DT; each dot represents one mouse ($n = 4$–5 mice per genotype). (**b**) Quantification of MCs in Giemsa-stained back skin after 4 i.p. injections of DT; bar = 200 μm, each dot represents one mouse ($n = 4$–5 mice per genotype). (**c**) DT injection regime during wound healing. (**d**) Upper panel, H&E-stained wound section at day 14 illustrating the distinct areas at the wound site; bar = 500 μm; lower panel, quantification of MCs in distinct areas of the wound site in Giemsa-stained sections; each dot represents one wound ($n = 6$–11 wounds from 3–6 mice per genotype and time point). (**e**) Representative Giemsa-stained wound sections at day 14; bar = 40 μm. Dotted line underlines hyperproliferative epithelium. d, dermis; DT, diphtheria toxin; e, epidermis; he, hyperproliferative epithelium; H&E, hematoxylin and eosin; iDTR, inducible diphtheria toxin receptor; MC, mast cell; Mcpt5, mast cell protease 5; pc, panniculus carnosus; sf, subcutaneous fat tissue; sm, skeletal muscle. $^{**}P < 0.01$, $^{***}P < 0.001$.

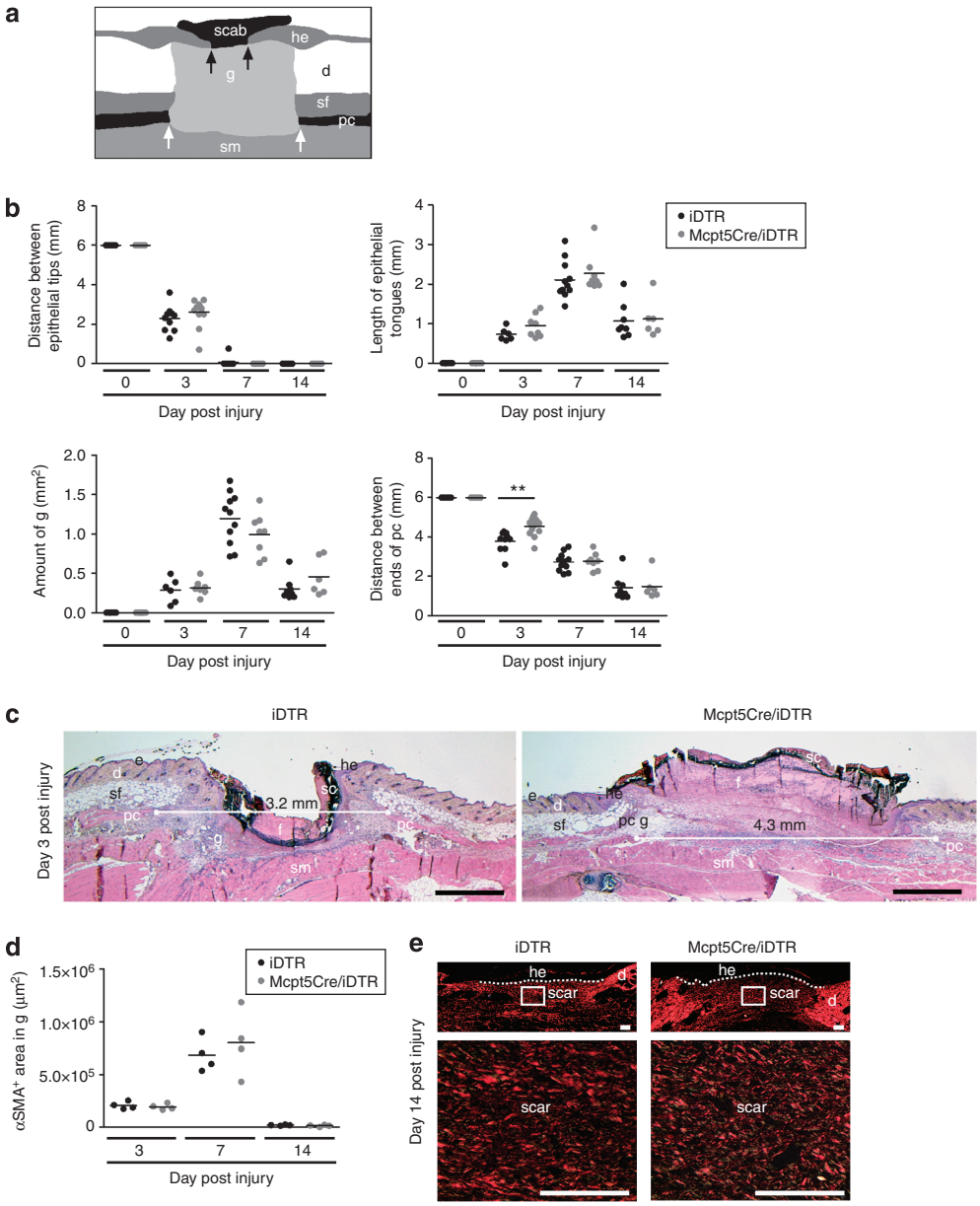

Figure 3. Severe reduction of MC numbers does not affect the repair of excision skin injury. (**a**) Scheme of a wound section following injury: black arrows indicate tips of the hyperproliferative epithelial tongues, and white arrows indicate ends of the panniculus carnosus. (**b**) Wound healing parameters in control and Mcpt5Cre/iDTR mice; each dot represents one wound ($n = 6$–11 wounds from 3 to 6 mice per genotype and time point), $^{**}P < 0.01$. (**c**) Representative H&E-stained wound sections from control and Mcpt5Cre/iDTR mice 3 days after injury; length between the two ends of the panniculus carnosus is depicted; bar = 1 mm. (**d**) Quantification of αSMA-positive area within the granulation tissue; each dot represents one wound ($n = 4$ wounds from 2 mice per genotype and time point). (**e**) Picrosirius red–stained wound sections at day 14 analyzed in polarized light; bar = 100 μm. d, dermis; e, epidermis; g, granulation tissue; he, hyperproliferative epithelium; H&E, hematoxylin and eosin; iDTR, inducible diphtheria toxin receptor; MC, mast cell; Mcpt5, mast cell protease 5; pc, panniculus carnosus; sf, subcutaneous fat tissue; sm, skeletal muscle; αSMA, α-smooth muscle actin.

within the late granulation tissue and contractile effects of the panniculus carnosus (Martin, 1997). The area of αSMA^+ myofibroblasts, the cellular correlate of granulation tissue contraction during skin repair, was similar in control and MC-depleted mice at 4 and 7 days after injury (Figure 3d).

MCs have been frequently associated with the development of tissue fibrosis. To examine the impact of MCs on scar development, we characterized the transition of late granulation tissue in scar tissue. Neither the amount of scar tissue was altered by MC depletion (Figure 3b) nor the number of $aSMA^+$ myofibroblasts within mid-stage granulation tissue in controls and MC-depleted animals (Figure 3d). Furthermore, as revealed by Picrosirius red staining and analysis in polarized light, MC ablation has no impact on the organization and fibrillar structure of collagen in scar formation after injury (Figure 3e). Notably, to investigate whether the few MCs still detectable in late-stage day 14 wounds in some DT-treated Mcpt5Cre/iDTR mice (average <15%), we performed

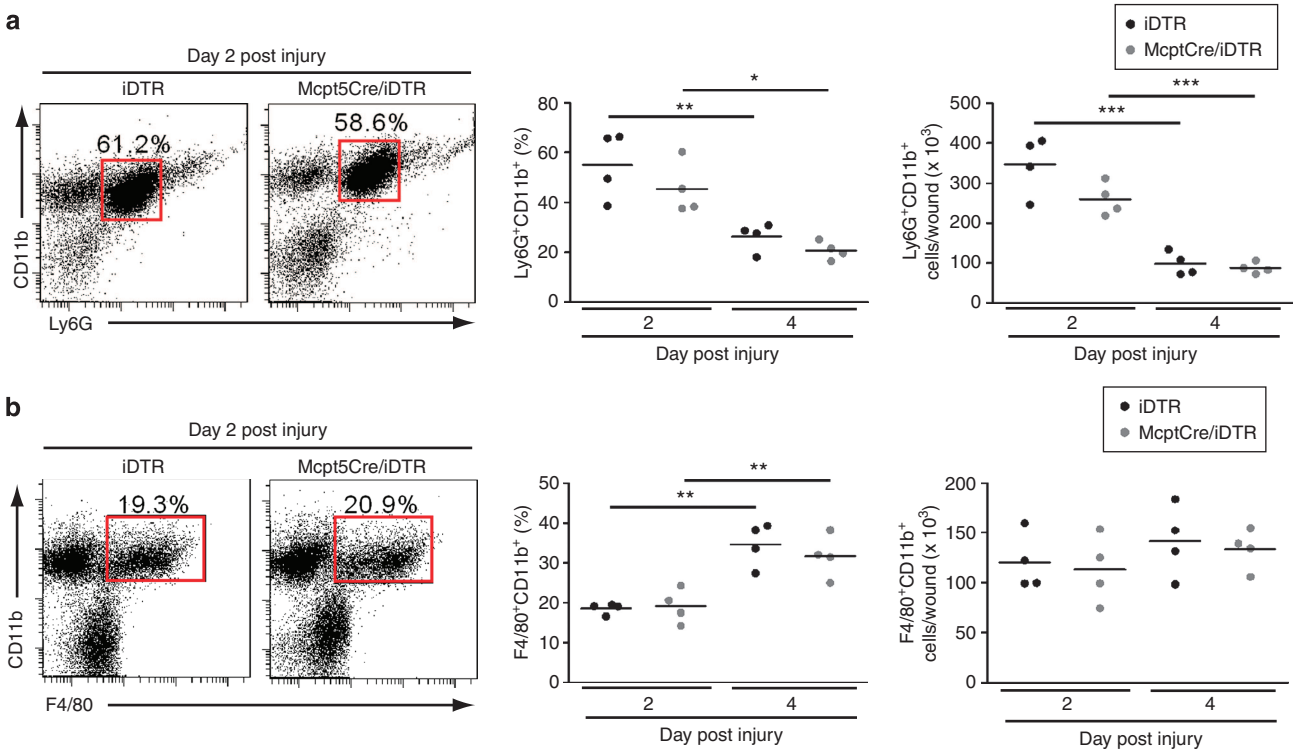

Figure 4. MCs do not critically affect the recruitment of inflammatory cells to the wound site. Single-cell suspensions isolated from wounds of control and Mcpt5Cre/iDTR mice were analyzed by flow cytometry. (**a**) 7-AAD$^-$ wound cells were gated and the frequency of neutrophils (Ly6G$^+$CD11b$^+$) was analyzed at time points as indicated; relative and absolute cell numbers are depicted; each dot represents one wound ($n=4$ wounds from 2 mice per genotype and time point). (**b**) 7-AAD$^-$ wound cells were gated and the frequency of macrophages (F4/80$^+$CD11b$^+$) was analyzed at time points as indicated; relative and absolute cell numbers are depicted. Two independent experiments were performed; each dot represents one wound ($n=4$ wounds from 2 mice per genotype and time point), $^*P<0.05$, $^{**}P<0.01$, $^{***}P<0.001$. 7-AAD, 7-Amino-Actinomycin D; iDTR, inducible diphtheria toxin receptor; MC, mast cell; Mcpt5, mast cell protease 5.

DT dosing experiments to correlate MC numbers with the healing response. Notably, neither a mild (42.3 ± 13.5%) nor a severe (85.4 ± 6.1%) reduction of wound MCs had any impact on epithelialization or scar formation (Figure 3b; Supplementary Figure S1B and C online).

Infiltration of leukocytes to the site of skin injury is not altered in MC-deficient mice

To characterize the impact of MCs on the composition of the early inflammatory infiltrate during skin repair, wound cell suspensions isolated from MC-depleted and control mice were analyzed by flow cytometry at days 2 and 4 after injury. In the wounds of both control and MC-depleted mice, the relative and absolute numbers of polymorphonuclear cells (Ly6G$^+$CD11b$^+$) significantly decreased from day 2 to 4 after injury (Figure 4a), whereas the relative number of macrophages (F4/80$^+$CD11b$^+$) significantly increased during this period (Figure 4b). Results from FACS analysis in wound tissues were confirmed by immunohistochemical stainings (data not shown). Both analyses showed that infiltration of leukocytes to the site of injury was not altered by MC depletion.

Genetic ablation of MCs fails to prevent bleomycin-induced skin fibrosis in mice

To investigate the functional impact of MCs on the development of skin fibrosis, the back skin of MC-depleted and control mice was challenged with repetitive i.d. injections of bleomycin. To maintain MC ablation over the time course of bleomycin challenge, i.p. DT injections were continued in weekly intervals (Figure 5a). Analysis of Giemsa-stained tissue sections in control mice revealed a major accumulation of MCs within fibrotic lesions (skin area with maximal dermal thickening) and within the adjacent skin (fibrotic edge Figure 5b). At both time points, the accumulation of MCs was more severe at the margins than within the fibrotic lesions itself in control mice (Figure 5b). MC depletion was highly efficient within fibrotic lesions and margins in DT-treated Mcpt5Cre/iDTR mice versus control mice over the time course of the experiment (Figure 5b).

To examine whether MC accumulation in skin during bleomycin challenge correlated with the development of skin fibrosis, hematoxylin and eosin–stained sections of fibrotic tissues from MC-depleted and control mice (iDTR mice treated with NaCl or bleomycin) were subjected to histological quantification. The findings revealed a massive increase of dermal thickening in fibrotic lesions of bleomycin-challenged control and MC-depleted mice at days 14 and 28 when compared with NaCl-treated control mice (Figure 6a and b).

Picrosirius red staining of tissue sections and analysis in polarized light showed that the collagen bundles within fibrotic lesions of bleomycin-treated mice appeared thicker (indicated by arrowheads), were densely packed, and had

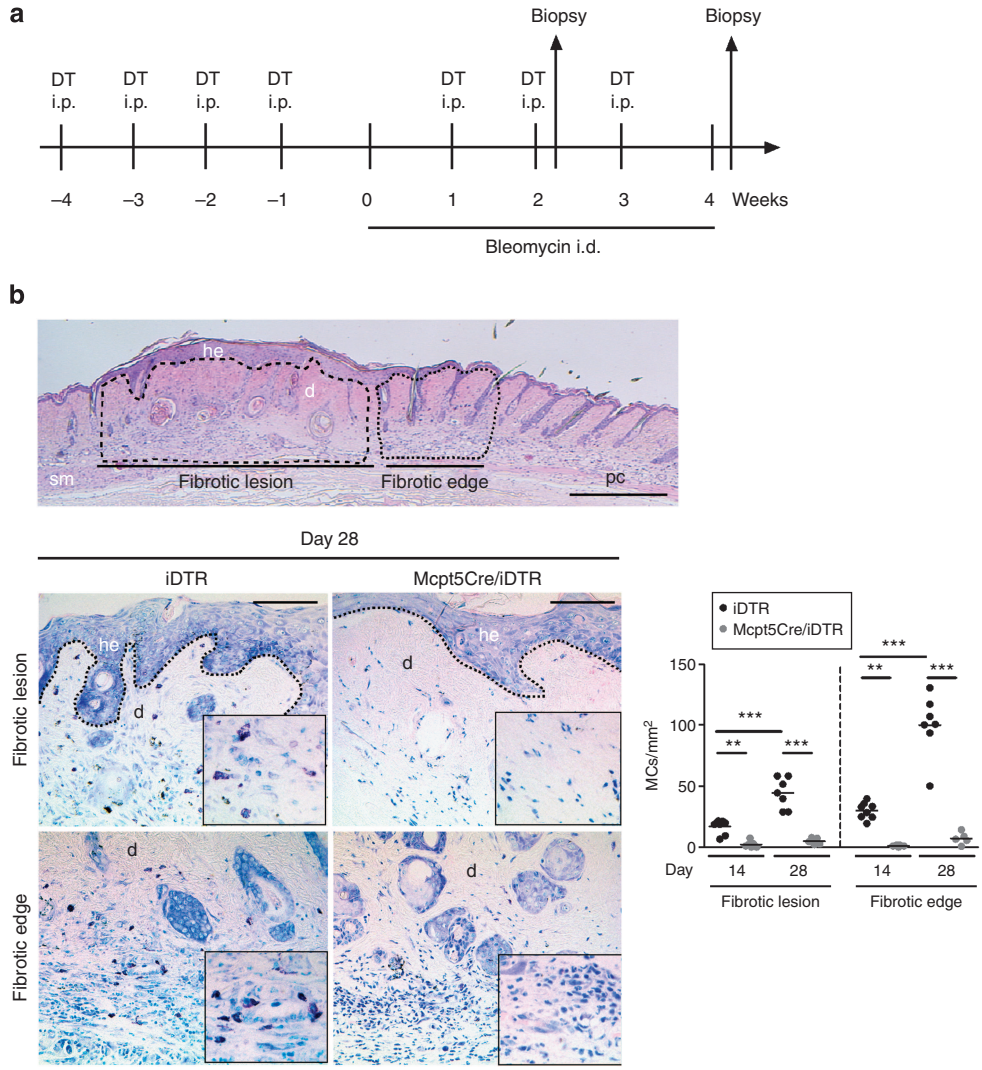

Figure 5. Efficient MC ablation in Mcpt5Cre/iDTR mice during bleomycin challenge. (**a**) DT injection regime during development of skin fibrosis. (**b**) Upper panel, scheme illustrating morphology of fibrotic tissue; hatched line indicates fibrotic lesion and dotted line indicates fibrotic edge; bar = 500 μm. Lower panel: MCs were analyzed within fibrotic lesions and fibrotic edges (not injected by bleomycin, histologically characterized by absence of dermal thickening, ~500 μm distant from the border of the bleomycin-injected lesion) of control and Mcpt5Cre/iDTR mice at indicated time points in Giemsa-stained sections; dotted line underlines hyperproliferative epithelium; bar = 100 μm. d, dermis; DT, diphtheria toxin; he, hyperproliferative epithelium; i.d., intradermally; iDTR, inducible diphtheria toxin receptor; MC, mast cell; Mcpt5, mast cell protease 5; pc, panniculus carnosus; sf, subcutaneous fat tissue; sm, skeletal muscle. Each dot represents the fibrotic lesion per mouse ($n = 5$–8 mice per group and time point). $^{**}P < 0.01$, $^{***}P < 0.001$.

typical red birefringence when compared with NaCl-treated mice, with no significant differences between control and MC-depleted mice (Figure 6c). We further assessed the biochemical nature of collagen fibril crosslinks formed in bleomycin-induced skin lesions in MC-depleted versus control mice. IL-4 has been shown to be a potent inducer of fibrosis-associated collagen crosslinks (Brinckmann *et al.*, 2005) and we speculated that MCs may be a source for IL-4 in fibrotic tissues. For this purpose, the amount of fibrosis-associated crosslinks hydroxylysyl pyridinoline and dihydroxylysinonorleucine and the amount of healthy skin–associated crosslinks histidino-hydroxylysinonorleucine and hydroxylysinonorleucine were determined in fibrotic tissue (Figure 6d). Findings revealed a robust increase in the ratio of hydroxylysyl pyridinoline and dihydroxylysinonorleucine to histidino-hydroxylysinonorleucine and hydroxylysinonorleucine within fibrotic lesions of control and MC-depleted mice when compared with untreated and NaCl-treated control skin (Figure 6d). No significant difference between control and MC-depleted mice was detected (Figure 6d).

DISCUSSION

The unresolved functional role of MCs in skin repair and fibrosis as well as the discovery of effects in $Kit^{W/Wv}$ mutants not related to their MC deficiency led us to initiate studies to reevaluate MC functions in skin repair and fibrosis. Here we used the recently developed MC-specific Mcpt5Cre mouse line to follow the kinetics and the spatial distribution of MCs accumulating at the site of skin damage in a Mcpt5Cre/eYFP reporter mouse model. Our analysis showed that MCs

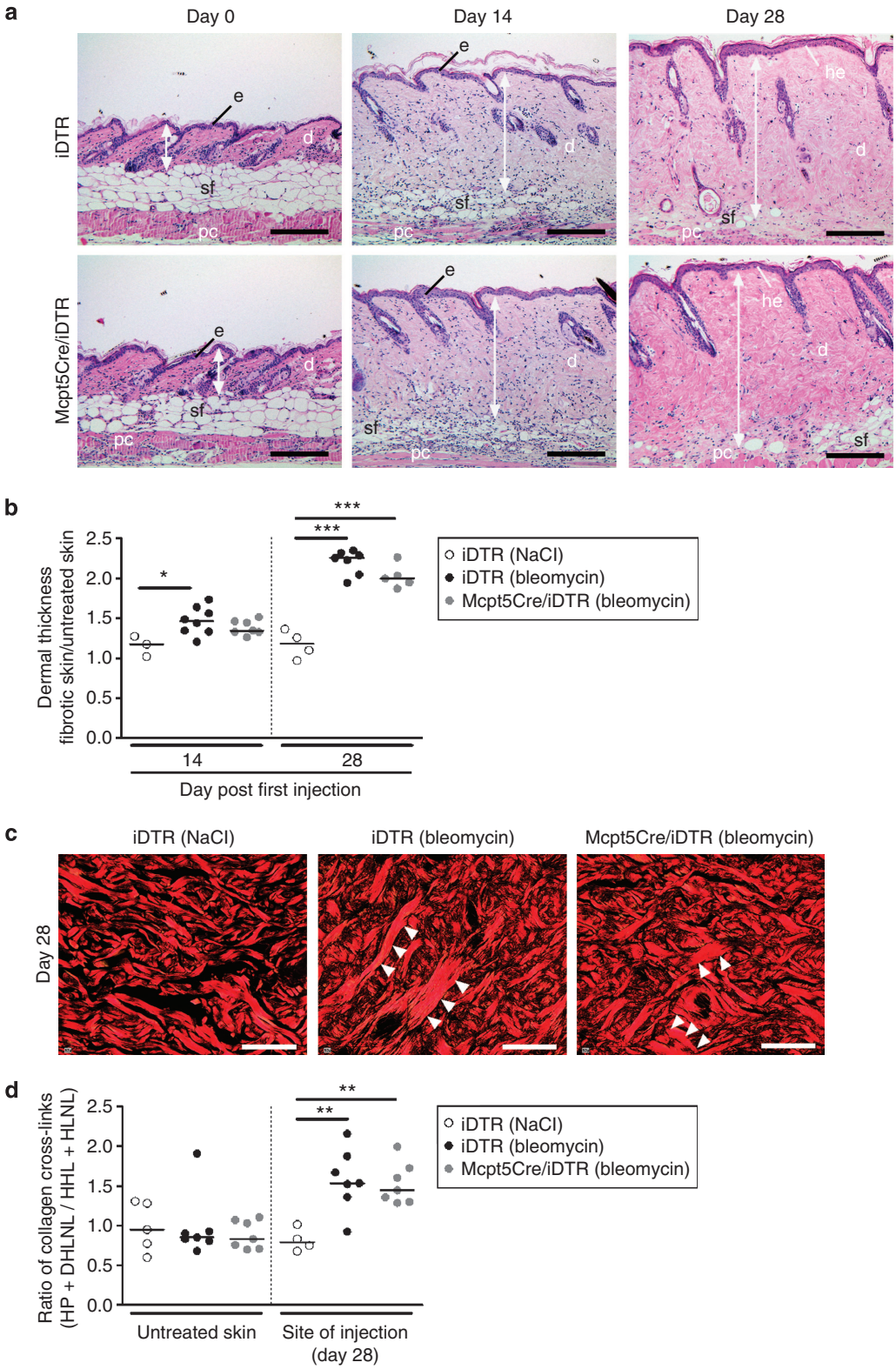

Figure 6. Genetic ablation of mast cells (MCs) fails to prevent skin fibrosis in mice. (**a**) Analysis of dermal thickness in bleomycin-induced fibrotic lesions (H&E stain). Arrows indicate dermal thickness; bar = 200 μm. (**b**) Quantification of dermal thickness in skin samples of mice treated as indicated. (**c**) Picrosirius red–stained and in polarized light analyzed skin sections; arrowheads indicate thick collagen bundles within fibrotic lesions; bar = 50 μm. (**d**) Analysis of collagen crosslink formation in skin samples; depicted is the ratio of HP + DHLNL to HHL + HLNL crosslinks. (**b**, **d**) Each dot represents the fibrotic lesion per mouse ($n = 3$–8 mice per group and time point). *$P<0.05$, **$P<0.01$, ***$P<0.001$. d, dermis; DHLNL, dihydroxylysinonorleucine; e, epidermis; he, hyperproliferative epidermis; H&E, hematoxylin and eosin; HHL, histidino-hydroxylysinonorleucine; HLNL, hydroxylysinonorleucine; HP, hydroxylysyl pyridinoline; pc, panniculus carnosus; sf, subcutaneous fat tissue.

accumulate both at the site of excision injury and repair and in bleomycin-induced fibrotic skin lesions. In both models, we found a distinct difference in the kinetic and the spatial distribution of MC accumulation between the actual site of skin injury/repair and the skin adjacent to the damaged lesion. Increased MC numbers are initially detectable particularly at the edge of the injured tissue, followed by an increase within the actual site of repair (granulation tissue) or fibrotic lesion. At this stage we can only speculate on the mechanism underlying this particular spatial distribution of MC accumulation following skin injury and restoration of tissue integrity. MCs in skin wounds might originate from MC precursors circulating in the blood stream as described by Rodewald *et al.* (1996). However, as *in vitro* studies suggest, in addition/alternatively, hair follicles that are present at wound margins may serve as a reservoir for skin MC precursors (Kumamoto *et al.*, 2003). We did not detect proliferating MCs at any stage of the healing response or in any area of the wound tissue (data not shown), supporting the concept of active recruitment of MC precursors into the wound site.

In this study we used the Mcpt5Cre mouse line to generate a mouse model of DT-inducible ablation of connective tissue–type MCs. We show that a combination of repetitive i.p. and i.d. DT injections leads to significant MC ablation during the processes of skin repair and bleomycin-induced skin fibrosis. Findings in the excision skin injury model convincingly showed that MC ablation did not critically affect wound closure kinetics. Hence, it is unlikely that the increased distance between the ends of the panniculus carnosus 3 days after injury in MC-depleted mice reflects reduced wound contraction due to attenuated myofibroblast differentiation. Our findings rather suggest that activated tissue-resident MCs located adjacent to the damaged skin release mediators that may act directly on the contractility of the panniculus carnosus. In rodents, contraction of the panniculus carnosus is supposed to contribute to overall wound closure (Galiano *et al.*, 2004), particularly during the early phase of repair. However, this process does not significantly contribute to the proliferative phase of the healing response (meaning effective tissue growth and cell proliferation). Furthermore, humans do not have a panniculus carnosus and contraction of this skin muscle is of minor importance when investigating repair mechanisms with potential clinical consequences.

Although here we show that connective tissue MCs can be virtually entirely ablated in nonchallenged skin in Mcpt5Cre/iDTR mice, in experimentally challenged skin lesions, minimal numbers of sporadic MCs were detectable during the late-stage healing response and bleomycin-induced fibrosis, and may raise the question of whether these residual MCs mediated the healing/fibrotic response. However, here we showed that neither a mild ($42.3 \pm 13.5\%$) nor a severe ($85.4 \pm 6.1\%$) reduction of MCs in the injured tissue affects the healing response, thereby arguing against this concern. In addition, recent studies, exploring skin repair in a different genetic mouse model of MC-ablation, did not detect significant alterations during the healing response in the absence of MCs (Antsiferova *et al.*, 2013; Nauta *et al.*, 2013). Furthermore, it is noteworthy to mention that in the previously studied W/W^v mice, few MCs are present in normal and, particularly, in inflamed skin (Waskow *et al.*, 2007; Feyerabend *et al.*, 2011). Collectively, these findings provide arguments that differences observed between W/W^v mice and the recently developed genetic mouse model are very likely to reflect non-MC-specific effects.

To test the hypothesis of whether MCs have nonredundant functions on the extent and/or the quality of fibrosis development, we employed two independent approaches. First, we analyzed formation of fibrosis in a physiological process, e.g., scar formation following excision skin injury and repair. Earlier *in vitro* studies have demonstrated that MC-derived mediators, in particular tryptase, exert profibrotic effects by stimulating proliferation and collagen synthesis in human fibroblasts isolated from various organs (Cairns and Walls, 1997; Kondo *et al.*, 2001; Garbuzenko *et al.*, 2002). Furthermore, systemic Ketotifen treatment has been shown to attenuate excessive scar contraction in excisional skin wounds in pigs, suggesting a role of MCs in wound-induced scar formation and contraction (Gallant-Behm *et al.*, 2008). Ketotifen is a well-known stabilizer of MCs, but more recently additional anti-inflammatory effects have been discussed that may affect scar formation (Lambiase *et al.*, 2009). Our studies indicate that the amount of scar tissue and the overall organization of collagen fibers were not altered in MC-depleted mice. Our findings are in line with observations by Egozi *et al.* (2003) reporting on similar hydroxyproline levels in scar tissue of control and $Kit^{W/Wv}$ mice. In contrast, Iba *et al.* (2004) report on higher levels of hydroxyproline in excision wounds of $Kit^{W/Wv}$ mice compared with controls, although the underlying mechanisms remain obscure in this study. Apart from a minor role of MC-derived mediators in the healing response, another possible explanation for nonaltered scar tissue in MC-depleted Mcpt5Cre/iDTR mice may be that the loss of profibrotic MC-derived mediators can be compensated by other (inflammatory and/or noninflammatory) cell types being more abundant at the wound site (e.g., macrophages). In addition, we also examined fibrosis development in a pathological condition, e.g., bleomycin-induced skin fibrosis. Bleomycin-induced skin fibrosis is a well-established disease model for skin sclerosis, although the basic mechanisms are not yet completely understood (Yamamoto and Nishioka, 2005). It is speculated that bleomycin provokes an inflammatory response inducing skin fibrosis (Yamamoto and Nishioka, 2005). As shown in this study and earlier by others, MCs accumulate in bleomycin-induced fibrosis and thus may contribute to its pathology (Yamamoto *et al.*, 1999a). Yamamoto *et al.* (1999b) challenged the skin of $Kit^{W/Wv}$ mice with bleomycin and showed that MCs are not required for the development of skin fibrosis. In our study we used the same model of bleomycin-induced skin fibrosis and did not detect any biochemical or structural difference in fibrosis development under conditions of severe reduction of MC numbers. Thus, our findings in MC-depleted Mcpt5Cre/iDTR mice corroborate the observation in $Kit^{W/Wv}$ mice that MCs do not affect the development of skin fibrosis in the examined physiological and pathological conditions in mice. However, we wish to point out that our findings cannot rule out that

alterations in scar formation that can be observed after months and years of injury in humans such as hypertrophic scars and keloids, or even fibrosis in other organs than the skin, e.g. the lung (Veerappan *et al.*, 2013), are at least in part mediated by MCs.

Conclusively, this study shows that the Mcpt5Cre/iDTR mouse represents a valuable model to study functions of MCs in skin repair and fibrosis *in vivo*. Although at this stage we cannot exclude that lack of MCs in Mcpt5Cre/iDTR mice may be compensated by factors released from other cell types, our findings provide strong evidence that severe reduction of tissue-resident MCs does not affect the proper kinetics of skin repair and the development of skin fibrosis. Thus, our findings point out to carefully revisit the concept of MCs as promising target for therapeutic intervention in wound healing or fibrotic pathologies.

MATERIALS AND METHODS

Mice

Mcpt5Cre/iDTR mice (Buch *et al.*, 2005; Scholten *et al.*, 2008) and Mcpt5Cre/eYFP reporter mice (Srinivas *et al.*, 2001) were generated and genotyped by PCR as described earlier. Mice were used at the age of 10–12 weeks and housed in specific pathogen-free conditions. Mcpt5Cre/iDTR and iDTR littermates received repetitive i.p. injections of 25 ng DT per g bodyweight (Sigma-Aldrich, St Louis, MO) as indicated. All procedures were in accordance with institutional guidelines on animal welfare and were approved by the North Rhine-Westphalia State Environment Agency, Germany.

Wounding and preparation of wound tissue

Wounding and preparation of wound tissue for histology was performed as recently described (Lucas *et al.*, 2010). Briefly, mice were anesthetized and full-thickness, circular wounds (6 mm punch biopsies) were created on the back. Mice were housed individually during the entire time course of healing. For histological analysis, wounds were excised at indicated time points after injury, bisected exactly in the center of the wound in caudocranial direction, and the tissue was either fixed overnight in 4% formalin or embedded in Optimal Cutting Temperature (OCT) compound (Sakura Finetek Europe B.V., Alphen aan den Rijn, The Netherlands); corresponding serial sections of wound tissue in controls and MC-depleted mice were compared. To assure exact and reproducible dissection in the center of the wound, wound edges were tattooed appropriately at the time of wounding. To increase MC ablation efficiency, Mcpt5Cre/iDTR and control mice received after injury one i.p. DT injection (day 2 after injury) and one i.d. DT injection at the wound edge (5 ng per wound in 50 µl phosphate-buffered saline) (day 9 after injury).

Induction of skin fibrosis by bleomycin

To evaluate the role of MCs during the development of skin fibrosis, we used an established scleroderma mouse model (Yamamoto *et al.*, 1999a). Mice received daily i.d. injections with 100 µg of bleomycin. Tissues were fixed in 4% formalin or embedded in OCT compound (Tissue Tek).

Flow cytometric analysis

Wound cells were isolated by a combination of enzymatic digestion (Liberase blendzyme, Roche Applied Science, Penzberg, Germany) and mechanical disruption (BD Medimachine System, BD Biosciences, San Diego, CA). For FACS analysis, Fc receptors were blocked with mouse seroblock FcR (CD16/CD32, eBioscience, San Diego, CA) and cells were stained with phycoerythrin-conjugated anti-IgE (eBioscience), allophycocyanin (APC)-conjugated anti-c-kit (eBioscience), phycoerythrin-conjugated anti-F4/80 (AbD Serotec, Oxford, UK), APC-conjugated anti-CD11b (Miltenyi Biotech, Bergisch Gladbach, Germany), APC-eFluor780-conjugated anti-CD45 (eBioscience), or APC-cyanine7-conjugated anti-Ly6G (BD Biosciences). Cells were incubated with antibodies (30 minutes, 4 °C) and washed 3 times thereafter in washing buffer (1% BSA, 2 mM EDTA in phosphate-buffered saline). Dead cells were excluded by using 7-Amino-Actinomycin D (BD Biosciences). Cells were analyzed using a FACSCanto II flow cytometer and the FACSDiva Software Version 6.1.1 (BD Biosciences).

Immunohistochemistry

Cryosections (10 µm) were fixed and incubated with primary (APC-conjugated anti-c-kit (eBioscience), anti-eYFP (Life Technologies, Carlsbad, CA), and Cy3-coupled anti-α-smooth muscle actin (Sigma)) and secondary (Alexa488-conjugated (Life Technologies)) antibodies. The 4′,6-diamidino-2-phenylindole serves as counterstain (Life Technologies). Images were acquired using Nikon Eclipse E800 and Olympus DeltaVision with NIS-Elements AR 2.30 Software (Nikon, Tokyo, Japan) or Softworx Suite 2.0 software (Olympus, Tokyo, Japan), processed with Adobe Photoshop 7.0 (Adobe Systems, San Jose, CA), and analyzed with ImageJ (Image Processing and Analysis in Java, National Institute of Mental Health, Bethesda, MD).

Morphometric analysis

Morphometric analysis was performed on hematoxylin and eosin–stained tissue sections using light microscopy (Leica DM4000B, Leica, Wetzlar, Germany) at indicated magnifications as recently described (Lucas *et al.*, 2010). Staining for α-smooth muscle actin was quantified in high-power fields ($7{,}000 \times 5{,}500\,\mu m^2$) within granulation tissue using ImageJ software. Analyses were performed in a blinded manner by two independent investigators.

Analysis of collagen crosslinks

Analysis of collagen crosslinks was performed using an amino acid analyzer (Biochrom 30, Merck Millipore, Darmstadt, Germany) as previously described (Brinkmann *et al.*, 2005) (for detailed information see Supplementary Material and Methods online).

Statistical analysis

Significance of difference was analyzed using Student's unpaired two-tailed *t*-test or analysis of variance one-way analysis with Tukey's multiple comparison test. Data are presented as means, and a *P*-value of <0.05 was considered significant. Significance levels are indicated in each figure.

CONFLICT OF INTEREST

The authors state no conflict of interest.

ACKNOWLEDGMENTS

We thank Michael Piekarek and Margot Junker for tissue sectioning and staining. This work was supported by the Deutsche Forschungsgemeinschaft (SFB829 to BE, TK, SAE; SFB832 to KH), CECAD (to TK and SAE), and CMMC (to TK and SAE).

SUPPLEMENTARY MATERIAL

Supplementary material is linked to the online version of the paper at http://www.nature.com/jid

REFERENCES

Antsiferova M, Martin C, Huber M *et al.* (2013) Mast cells are dispensable for normal and activin-promoted wound healing and skin carcinogenesis. *J Immunol* 191:6147–55

Brinckmann J, Kim S, Wu J *et al.* (2005) Interleukin 4 and prolonged hypoxia induce a higher gene expression of lysyl hydroxylase 2 and an altered cross-link pattern: important pathogenetic steps in early and late stage of systemic scleroderma? *Matrix Biol* 24:459–68

Buch T, Heppner FL, Tertilt C *et al.* (2005) A Cre-inducible diphtheria toxin receptor mediates cell lineage ablation after toxin administration. *Nat Methods* 2:419–26

Cairns JA, Walls AF (1997) Mast cell tryptase stimulates the synthesis of type I collagen in human lung fibroblasts. *J Clin Invest* 99:1313–21

Dudeck A, Dudeck J, Scholten J *et al.* (2011) Mast cells are key promoters of contact allergy that mediate the adjuvant effects of haptens. *Immunity* 34:973–84

Egozi EI, Ferreira AM, Burns AL *et al.* (2003) Mast cells modulate the inflammatory but not the proliferative response in healing wounds. *Wound Repair Regen* 11:46–54

Eming SA, Krieg T, Davidson JM (2007) Inflammation in wound repair: molecular and cellular mechanisms. *J Invest Dermatol* 127:514–25

Feyerabend TB, Weiser A, Tietz A *et al.* (2011) Cre-mediated cell ablation contests mast cell contribution in models of antibody- and T cell-mediated autoimmunity. *Immunity* 35:832–44

Gabrielli A, Avvedimento EV, Krieg T (2009) Scleroderma. *N Engl J Med* 360:1989–2003

Gallant-Behm CL, Hildebrand KA, Hart DA (2008) The mast cell stabilizer ketotifen prevents development of excessive skin wound contraction and fibrosis in red Duroc pigs. *Wound Repair Regen* 16:226–33

Galiano RD, Michaels J 5th, Dobryansky M *et al.* (2004) Quantitative and reproducible murine model of excisional wound healing. *Wound Repair Regen* 12:485–92

Garbuzenko E, Nagler A, Pickholtz D *et al.* (2002) Human mast cells stimulate fibroblast proliferation, collagen synthesis and lattice contraction: a direct role for mast cells in skin fibrosis. *Clin Exp Allergy* 32:237–46

Gurtner GC, Werner S, Barrandon Y *et al.* (2008) Wound repair and regeneration. *Nature* 453:314–21

Iba Y, Shibata A, Kato M *et al.* (2004) Possible involvement of mast cells in collagen remodeling in the late phase of cutaneous wound healing in mice. *Int Immunopharmacol* 4:1873–80

Kitamura Y, Go S, Hatanaka K (1978) Decrease of mast cells in W/Wv mice and their increase by bone marrow transplantation. *Blood* 52:447–52

Kondo S, Kagami S, Kido H *et al.* (2001) Role of mast cell tryptase in renal interstitial fibrosis. *J Am Soc Nephrol* 12:1668–76

Kumamoto T, Shalhevet D, Matsue H *et al.* (2003) Hair follicles serve as local reservoirs of skin mast cell precursors. *Blood* 102:1654–60

Lambiase A, Micera A, Bonini S (2009) Multiple action agents and the eye: do they really stabilize mast cells? *Curr Opin Allergy Clin Immunol* 9:454–65

Lucas T, Waisman A, Ranjan R *et al.* (2010) Differential roles of macrophages in diverse phases of skin repair. *J Immunol* 184:3964–77

Martin P (1997) Wound healing-aiming for perfect skin regeneration. *Science* 276:75–81

Nauta AC, Grova M, Montoro DT *et al.* (2013) Evidence that mast cells are not required for healing of splinted cutaneous excisional wounds in mice. *PLoS One;* published online 27 March 2013; doi:10.1371/journal.pone.0059167

Nigrovic PA, Gray DH, Jones T *et al.* (2008) Genetic inversion in mast cell-deficient (Wsh) mice interrupts corin and manifests as hematopoietic and cardiac aberrancy. *Am J Pathol* 173:1693–701

Rodewald HR, Dessing M, Dvorak AM *et al.* (1996) Identification of a committed precursor for the mast cell lineage. *Science* 271:818–22

Scholten J, Hartmann K, Gerbaulet A *et al.* (2008) Mast cell-specific Cre/loxP-mediated recombination in vivo. *Transgenic Res* 17:307–15

Sen CK, Gordillo GM, Roy S *et al.* (2009) Human skin wounds: a major and snowballing threat to public health and the economy. *Wound Repair Regen* 17:763–71

Srinivas S, Watanabe T, Lin CS *et al.* (2001) Cre reporter strains produced by targeted insertion of EYFP and ECFP into the ROSA26 locus. *BMC Dev Biol* 1:4

Trautmann A, Toksoy A, Engelhardt E *et al.* (2000) Mast cell involvement in normal human skin wound healing: expression of monocyte chemoattractant protein-1 is correlated with recruitment of mast cells which synthesize interleukin-4 in vivo. *J Pathol* 190:100–6

Veerappan A, O'Connor NJ, Brazin J *et al.* (2013) Mast cells: a pivotal role in pulmonary fibrosis. *DNA Cell Biol* 32:206–18

Wadman M (2005) Scar prevention: the healing touch. *Nature* 436:1079–80

Waskow C, Bartels S, Schlenner SM *et al.* (2007) Kit is essential for PMA-inflammation-induced mast-cell accumulation in the skin. *Blood* 109:5363–70

Weller K, Foitzik K, Paus R *et al.* (2006) Mast cells are required for normal healing of skin wounds in mice. *FASEB J* 20:2366–8

Wulff BC, Parent AE, Meleski MA *et al.* (2012) Mast cells contribute to scar formation during fetal wound healing. *J Invest Dermatol* 132:458–65

Yamamoto T, Takagawa S, Katayama I *et al.* (1999a) Animal model of sclerotic skin. I: Local injections of bleomycin induce sclerotic skin mimicking scleroderma. *J Invest Dermatol* 112:456–62

Yamamoto T, Takahashi Y, Takagawa S *et al.* (1999b) Animal model of sclerotic skin. II. Bleomycin induced scleroderma in genetically mast cell deficient WBB6F1-W/W(V) mice. *J Rheumatol* 26:2628–34

Yamamoto T, Nishioka K (2005) Cellular and molecular mechanisms of bleomycin-induced murine scleroderma: current update and future perspective. *Exp Dermatol* 14:81–95

Zhou JS, Xing W, Friend DS *et al.* (2007) Mast cell deficiency in Kit(W-sh) mice does not impair antibody-mediated arthritis. *J Exp Med* 204: 2797–802